

1 Evaluation of efficiency and sensitivity of 1D and 2D sample 2 pooling strategies for SARS-CoV-2 RT-qPCR screening purposes

3 Running title: *Evaluation of SARS-CoV-2 RT-qPCR pooling*

4 **Jasper Verwilt^{1,2,3}, Jan Helleman⁴, Tom Sante^{2,3}, Pieter Mestdag^{1,2,3,4}, Jo
5 Vandesompele^{1,2,3,4}**

6 *1 OncoRNALab, Cancer Research Institute Ghent, Corneel Heymanslaan 10, 9000
7 Ghent, Belgium*

8 *2 Department of Biomolecular Medicine, Ghent University, Corneel Heymanslaan 10,
9 9000 Ghent, Belgium*

10 *3 Center for Medical Genetics, Ghent University, Corneel Heymanslaan 10, 9000
11 Ghent, Belgium*

12 *4 Biogazelle, Technologiepark 82, 9052 Zwijnaarde, Belgium*

13

14 • 17 text pages

15 • 4 figures

16

17 Corr. author:

18 Jo Vandesompele

19 Corneel Heymanslaan 10, 9000 Gent, Belgium

20 +32 9 332 55 32

21 jo.vandesompele@ugent.be

22

23 Funding: UGent BOF-GOA LNCCA (BOF16/GOA/023, J.Va.)

24

25 **Abstract**

26 To increase the throughput, lower the cost, and save scarce test reagents,
27 laboratories can pool patient samples before SARS-CoV-2 RT-qPCR testing. While
28 different sample pooling methods have been proposed and effectively implemented
29 in some laboratories, no systematic and large-scale evaluations exist using real-life
30 quantitative data gathered throughout the different epidemiological stages. Here, we
31 use anonymous data from 9673 positive cases to simulate and compare 1D and 2D
32 pooling strategies. We show that the optimal choice of pooling method and pool size
33 is an intricate decision with a testing population-dependent efficiency-sensitivity
34 trade-off and present an online tool to provide the reader with custom real-time
35 pooling strategy recommendations.

36 Introduction

37 One of the key strategies in the global battle against the COVID-19 pandemic is
38 massive population testing. However, an ongoing shortage of time, reagents and
39 testing capacity has tempered these efforts. Pooled testing of samples presents itself
40 as a valid strategy to overcome these hurdles and to realize rapid, large-scale testing
41 at lower cost and lower dependence on test reagents.

42

43 Multiple recent studies discussed pooling strategies in the frame of SARS-CoV-2
44 testing. Researchers have explored many strategies, but two of them have been
45 welcomed for their simplicity and effectiveness: one-time pooling (1D pooling) and
46 two-dimensional pooling (2D pooling). In 1D pooling, the samples are pooled, pools
47 are tested and samples in positive pools are tested individually (Figure 1)¹⁻⁴. Labs
48 worldwide have extensively evaluated 1D pooling strategies for SARS-CoV-2 testing
49 in the lab⁵⁻⁸ or using simulations¹. In 2D pooling, samples are organized in a 2D
50 matrix and pools are created along the matrix's rows and columns. The pools are
51 tested, and negative rows and columns are excluded from the matrix. Next, all
52 remaining samples are tested individually (Figure 1)⁹. Other more complex strategies
53 exist, such as repeated pooling¹, P-BEST¹⁰ and Tapestry¹¹.

54

55 While attractive, pooling strategies come with inherent limitations. First, pooling
56 dilutes each sample, possibly to such an extent that the viral RNA becomes
57 undetectable, which results in false negative observations^{8,9,12}. A second limitation is
58 that an increase in sample manipulations augments the risk of cross-contamination
59 and sample mix-ups, possibly leading to false negatives and false positives⁹. Last,
60 when pooling, identifying individual positive samples will take an additional RNA

61 extraction and RT-qPCR run, while one run is sufficient when testing individual
62 samples without pooling.

63

64 Although the number of preprints and peer-reviewed publications on pooling
65 strategies for COVID-19 RT-qPCR-based testing has accelerated rapidly throughout
66 the pandemic, some critical aspects remain mostly ignored. First of all, the proposed
67 optimal pooling strategy is most often based on a binary classification of samples as
68 either positive or negative. This Boolean approach is not true to the real-world
69 situation and does not investigate the pooling step's dilution effect. Second, when
70 using Cq values as a semi-quantitative measure¹³ of the viral loads, their overall
71 distribution should reflect the real-life population. A high fraction of Cq values close to
72 the limit of detection of the RT-qPCR assay produces an elevated risk of resulting in
73 false negative samples¹⁴. Last, since the Cq distribution of the sample population and
74 prevalence may vary over time, it remains unclear how the pooling strategy's
75 performance evolves as the pandemic progresses.

76

77 We questioned to what extent optimal pooling strategies would have changed
78 throughout the COVID-19 pandemic and how testing facilities might use pooling
79 strategies for future testing in a correct and attainable manner. To this extent, we
80 simulated and evaluated one-dimensional (1D) and two-dimensional (2D) pooling
81 strategies with different pool sizes using real-life RT-qPCR data gathered by the
82 Belgian national testing platform during the end of the first and the beginning of the
83 second SARS-CoV-2 epidemiological waves. Additionally, we formulate a detailed
84 action plan to provide testing laboratories with the most suitable pooling strategy
85 assuring an optimal efficiency-sensitivity trade-off.

86

87 **Materials and Methods**

88 *Patient samples*

89 Nasopharyngeal swabs were taken by a healthcare professional as a diagnostic test
90 for SARS-CoV-2, as part of the Belgian national testing platform. The individuals
91 were tested at nursing homes or in triage centers, between April 9th and June 7th, and
92 between September 1st and November 10th. After filtering the data as described
93 further, this resulted in 207 944 patients in total, of which 9673 positives (4.65%).

94

95 *SARS-CoV-2 RT-qPCR test*

96 During the first (spring) wave, RNA extraction was performed using the Total RNA
97 Purification Kit (Norgen Biotek #24300) according to the manufacturer's instructions
98 using 200 µl transport medium, 200 µl lysis buffer and 200 µl ethanol, with
99 processing using a centrifuge (5810R with rotor A-4-81, both from Eppendorf). RNA
100 was eluted from the plates using 50 µl elution buffer (nuclease-free water), resulting
101 in approximately 45 µl eluate. RNA extractions were simultaneously performed for 94
102 patient samples and 2 negative controls (nuclease-free water). After addition of the
103 lysis buffer, 4 µl of a proprietary 700 nucleotides spike-in control RNA (prior to May
104 25th, 40 000 copies for singleplex RT-qPCR; from May 25th onwards, 5000 copies for
105 duplex RT-qPCR) and carrier RNA (200 ng of yeast tRNA, Roche #10109517001)
106 was added to all 96 wells from the plate. To the eluate of one of the negative control
107 wells, 7500 RNA copies of positive control RNA (Synthetic SARS-CoV-2 RNA
108 Control 2, Twist Biosciences #102024) were added. During the second (autumn)
109 wave, RNA extraction was performed using the Quick-RNA Viral 96 Kit (Zymo
110 Research #R1041), according to the manufacturer's instructions using 100 µl

transport medium, with processing using a centrifuge (5810R with rotor A-4-81, both from Eppendorf). RNA was eluted from the plates using 30 µl elution buffer (nuclease-free water). RNA extractions were simultaneously performed for 92 patient samples, 2 negative controls (nuclease-free water), and 2 positive controls (1 diluted positive case as a full workflow control; 1 positive control RNA as RT-qPCR control, see further). After addition of the lysis buffer, 4 µl of a proprietary 700 nucleotides spike-in control RNA (5000 copies) and carrier RNA (200 ng of yeast tRNA, Roche #10109517001) was added to all 96 wells from the plate. To the eluate of one of the negative control wells, 7500 RNA copies of positive control RNA (Synthetic SARS-CoV-2 RNA Control 2, Twist Biosciences #102024) were added.

Six µl of RNA eluate was used as input for a 20 µl RT-qPCR reaction in a CFX384 qPCR instrument using 10 µl iTaq one-step RT-qPCR mastermix (Bio-Rad #1725141) according to the manufacturer's instructions, using 250 nM final concentration of primers and 400 nM of hydrolysis probe. Primers and probes were synthesized by Integrated DNA Technologies using clean-room GMP production. For detection of the SARS-CoV-2 virus, the Charité E gene assay was used (FAM)¹⁵; for the internal control, a proprietary hydrolysis probe assay (HEX) was used. Prior to May 25th, 2 singleplex assays were performed; from May 25th onwards, 1 duplex RT-qPCR was performed. Cq values were generated using the FastFinder software v3.300.5 (UgenTec). Only batches were approved with a clean negative control and a positive control in the expected range.

Digital PCR calibration of positive control RNA

Digital PCR was done on a QX200 instrument (Bio-Rad) using the One-Step RT-ddPCR Advanced Kit for Probes (Bio-Rad #1864022) according to the

manufacturer's instructions. Briefly, 22 μ l pre-reactions were prepared consisting of 5 μ l 4x supermix, 2 μ l reverse transcriptase, 6 μ l positive control RNA (125 RNA copies/ μ l), 15 mM dithiothreitol, 900 nM of each forward and reverse primer and 250 nM *E* gene hydrolysis probe (FAM) (see higher). 20 μ l of the pre-reaction was used for droplet generation using the QX200 Droplet Generator, followed by careful transfer to a 96-well PCR plate for thermocycling: 60 min 46 °C reverse transcription, 10 min 95 °C enzyme activation, 40 cycles of 30 sec denaturation at 95 °C and 1 min annealing/extension at 59 °C, and finally 10 min 98 °C enzyme deactivation. Droplets were analyzed by the QX200 Droplet Reader and QuantaSoft software. With an RNA input of 7500 copies per reaction, the digital PCR result was 1500 cDNA copies (or 20% of the expected number, a fraction confirmed by Dr. Jim Huggett for particular lot numbers of #102024, personal communication). The median Cq value of the positive control RNA of 24.55 thus corresponds to 1500 digital PCR calibrated cDNA molecules.

Determination of efficiency and sensitivity for simulated of 1D and 2D pooling strategies

Simulations are run using R 4.0.1. First, several cohorts of 100 000 patients are repeatedly simulated with varying fractions of positive cases f , depending on the fraction of positive samples of the investigated week. This is done five times, resulting in five replicate cohorts per week. The Cq values of the positive samples are sampled with replacement from the set of the positive Cq values of said week. Next, the patients are randomly separated into pools depending on the pooling strategy that is simulated. The pooling strategies that were simulated are 1x4, 1x8,

160 1x12, 1x16, 1x24 (all 1D), and 8x12, 12x16 and 16x24. The Cq value of the pool was
161 calculated as follows:

162

$$c_{pool} = \log_2 P - \log_2 \sum_{i=1}^p 2^{-c_i} \quad \#(1)$$

163

164

165 With c_{pool} the Cq value of the pool, P the number of samples in the pool, p the
166 number of positive samples in the pool, c_1, c_2, \dots, c_p the Cq values of the positive
167 samples. If the Cq value of the pool is lower than the single-molecule Cq value, it is
168 classified as a positive pool. For 1D pooling, only samples in positive pools are
169 retained and the remaining individual Cq values were checked to be positive. For 2D
170 pooling, the Cq values of the differently sized pools are checked simultaneously and
171 the samples in negative pools are removed, after which all Cq values of the
172 remaining samples are checked individually. Samples that were retained after the
173 testing of the pools and that had an individual Cq lower than the single-molecule Cq
174 value are classified as positive, all other samples are classified as negative.

175 The sensitivity is calculated as:

176

$$sensitivity = \frac{no. \text{ true positive samples}}{no. \text{ true positive samples} + no. \text{ false negative samples}} \quad \#(2)$$

177

178

179 The analytical efficiency gain is calculated as:

180

$$efficiency\ gain = \frac{no.\ tests\ required\ for\ individual\ testing}{no.\ tests\ required\ for\ pooling\ strategy} \#(3)$$

In all simulations, the number of tests required for individual testing is equal to the number of samples (assuming no technical failures). The outcomes for each simulation were identical as the sample size far outreached the size of the dataset. The code is available at <https://github.com/OncoRNALab/covidpooling>.

Ad hoc sensitivity and efficiency calculation

To calculate the efficiency for a specific 1D pooling strategy on a real sample set, the following equation was used:

$$efficiency = \frac{n}{\frac{n}{s} \cdot (1 + s \cdot \sum_{k=1}^s \left(\frac{s!}{k!(s-k)!} \cdot p^k \cdot (1-p)^{s-k} \cdot (1-c^k) \right))} \#(4)$$

With sample size n , pool size s , fraction of positive samples p and fraction of Cq values of positive samples above the 'dilution detection limit': the lowest individual Cq value that can result in a pooled Cq value lower than the single molecule Cq value, or:

$$single\ molecule\ Cq\ value - \log_2(pool\ size) \#(5)$$

Equation (4) is derived as follows. The efficiency is defined by the following equation:

$$efficiency = \frac{n}{no.\ tests\ required\ for\ pooling\ strategy} \#(6)$$

The number of tests performed when using a pooling strategy is equal to:

$$no.\ tests\ required\ for\ pooling\ strategy = no.\ pools + no.\ positive\ pools \cdot s \#(7)$$

200

201 Since $\# pools = \frac{n}{s}$,

$$no. tests required for pooling strategy = \frac{n}{s} + no. positive pools \cdot s \# (8)$$

202 The exact number of positive pools can be calculated by multiplying the number of
203 pools by the probability of a pool testing positive. Approximately, a pool will test
204 positive if it includes a positive sample with a Cq value lower than the 'dilution
205 detection limit'. The probability of having a specific number of positive samples k in a
206 pool with pool size s is defined by a binomial distribution:

$$\frac{s!}{k! (s-k)!} \cdot p^k \cdot (1-p)^{s-k} \# (8)$$

207

208 Thus, the probability of having at least one positive value in a pool is equal to:

$$\sum_{k=1}^s \left(\frac{s!}{k! (s-k)!} \cdot p^k \cdot (1-p)^{s-k} \right) \# (10)$$

209

210 In general, we can assume that when a sample has a Cq value higher than the
211 'dilution detection limit', for the sample to test positive, it must be accompanied by a
212 sample with a Cq value lower than the 'dilution detection limit'. Equation (10) can be
213 adjusted to factor for these events:

$$\sum_{k=1}^s \left(\frac{s!}{k! (s-k)!} \cdot p^k \cdot (1-p)^{s-k} \cdot (1-c^k) \right) \# (10)$$

214

215 Filling in Eq. (10) in Eq. (8) results in the final formula being used for the calculation
216 of the efficiency.

217

218 To estimate the sensitivity for a specific 1D pooling strategy on a real sample set, the
219 following equation was used:

$$sensitivity = c \cdot \sum_{k=0}^{s-1} \left(\frac{(s-1)!}{k! ((s-1)-k)!} \cdot p^k \cdot (1-p)^{(s-1)-k} \cdot (1-c^k) \right) + (1-c) \quad \#(11)$$

220

221 The sensitivity can be defined as the probability a true positive sample tests positive.

222 For our situation it will be equal to the probability that any sample tests positive:

$$P(pos\ test) = P(pos\ test|Cq \geq\ cut\ off) \cdot P(Cq \geq\ cut\ off) + P(pos\ test|Cq <\ cut\ off) \cdot P(Cq <\ cut\ off) \quad \#(12)$$

223

224 Previously, $P(Cq \geq\ cut\ off)$ was defined as c and therefore $P(Cq <\ cut\ off) = 1 - c$.

225 Also $P(pos\ test|Cq <\ cut\ off) = 1$. A positive sample with Cq value above the

226 'dilution detection limit' can only test positive if one of the other samples in the pool is

227 also positive and has a Cq value lower than the 'dilution detection limit'. We can

228 calculate the probability of this happening by using the same logic as before, but with

229 $s - 1$ instead of s :

$$\sum_{k=0}^{s-1} \left(\frac{(s-1)!}{k! ((s-1)-k)!} \cdot p^k \cdot (1-p)^{(s-1)-k} \cdot (1-c^k) \right) \quad \#(13)$$

230

231 Completing Eq. (12) with Eq. (13) leads to Eq. (11) for calculating the sensitivity.

232

233 *Shiny application*

234 To help laboratories find the best pooling strategy for their specific situation (i.e. the

235 local positivity ratio and Cq value distribution), we developed a Shiny application in R

236 4.0.1. The Shiny application was launched on our in-house Shiny server and is

237 available at <https://shiny.dev.cmgg.be/>.

238

239

240 **Results**

241 *Single-molecule Cq value determination*

242 We made a 5-point 10-fold serial dilution series of positive control RNA from 150 000
243 (digital PCR calibrated) copies down to 15 copies. The Y-intercept value points at a
244 single-molecule Cq value of 35.66 and 35.28 for singleplex and duplex RT-qPCR,
245 respectively (Supplemental Figure 1). Therefore, we conservatively use 37 as the
246 single-molecule value for further analysis. Patient sample Cq values higher than the
247 single-molecule Cq value threshold are likely due to random measurement variation,
248 lot reagent variability and sample inhibition.

249

250 *Cq distribution is dynamic over course of the pandemic*

251 Few studies have explored how the Cq value distribution within one testing facility
252 evolves during the COVID-19 pandemic. We determined the 75%-tile of the Cq value
253 distribution and the percentage of positive tests per day as a proxy for actual Cq
254 value distribution and prevalence, respectively (Figure 2). We compared the fraction
255 of positive tests in our dataset with the fraction of positive tests as reported by the
256 federal agency for public health Sciensano (<https://epistat.wiv-isp.be/covid/>.
257 accessed January 25th, 2021). First, the fractions of positive tests seem to align at
258 the end of the first wave, but in the second wave our data seems to be shifted about
259 one to two weeks later. Second, the 75%-tile of the Cq values varies over the course
260 of the pandemic from a minimum value of around 18 and a maximum value of almost
261 35. Third, when comparing the fraction of positive samples and the 75%-tile of the Cq
262 value distribution, we note that these parameters are inversely related: when the

positivity rate goes down, the Cq value distribution shifts towards the higher end of the spectrum. In conclusion, the Cq value distribution and prevalence show a dynamic profile over the course of the COVID-19 pandemic. These observations are crucial considering that positivity rate and Cq value distribution are key determinants of efficiency and sensitivity of any pooling strategy.

Pooling efficiency and sensitivity changes as pandemic progresses

To explore how hypothetical pooling strategies would have affected the SARS-CoV-2 testing outcomes, we simulated different 1D (with pool size of 4, 8, 12, 16 and 24) and 2D pooling (with pool sizes of 8x12, 12x16, and 16x24) strategies using individual sample Cq values from a single Belgian laboratory during the end of the first and beginning of the second wave. The data was grouped by week and the resulting Cq value distributions and positivity rates were used as input for the simulations (Figure 3). First, sensitivity and efficiency show very opposing patterns when comparing different timeframes during the pandemic. At the end of the first wave the efficiency increases, while at the beginning of the second wave, the efficiency decreases. The sensitivity drops as we move further away from the first wave but remains stable as we enter the second. Second, pool size and strategy have a major influence on the outcomes. 2D pooling strategies generally have the highest efficiency, but the lowest sensitivity. Curiously, strategies with larger pool sizes were more efficient during the end of the first wave, but less efficient during the beginning of the second wave. The sensitivity was always higher for strategies with smaller pool sizes, irrespective of the time during the pandemic. We conclude that—just like the positivity rate and the Cq value distribution—the sensitivity and efficiency

depend on the timing in the pandemic and are heavily affected by the pooling strategy and the size of the pools.

Positivity rate drives efficiency, Cq distribution drives sensitivity

We wondered how the positivity rate, Cq value distribution and pooling strategy affect the performance of the adopted strategy. To investigate this, we used the previous simulations for the end of the first wave to create an adjusted visualization where all parameters involved are incorporated (Figure 4). First, it is apparent that weeks with a high 75%-tile Cq value tend to have a low sensitivity and weeks with a high positivity rate seem to have a low efficiency. Second, pooling strategies with smaller pool sizes seem less sensitive to changes in positivity rate and Cq value distribution, as indicated by the area of the polygon traced around the edges of the data (Figure 4). These results show that the prevalence mainly contributes to the efficiency and the Cq distribution to the sensitivity.

Shiny app for guided decision making

To provide laboratories with a custom pooling strategy recommendation based on their specific sampling population, we worked out equations to estimate the sensitivity and efficiency (for 1D pooling strategies) based on an uploaded dataset of Cq values. The derivation of these equations can be found in the Methods section. We focused on 1D pooling strategies since 2D pooling strategies generally resulted in extreme outcomes (highest efficiency and lowest sensitivity) and the outcomes of the optimal pooling strategy are situated somewhere in two extremes. To evaluate the equations' capacities to replicate the simulations, we compared the simulated efficiency and sensitivity of the pooling strategies for the different weeks and the

efficiency and sensitivity of the pooling strategies the distributions, fraction of positive samples and single-molecule cutoff as inputs for the formulas (Supplemental Figure 2 and Supplemental Figure 3). We integrated these formulas into an open-access Shiny application (Supplemental Figure 4). The application requires three inputs: a dataset of Cq values from positive samples, the positivity rate and the single-molecule cut-off Cq value. The Shiny application will then swiftly output the estimated data-specific efficiency and sensitivity for different pooling strategies.

Discussion

Using a sizeable real-life dataset of 9673 SARS-CoV-2 positive nasopharyngeal samples, we found that the pooling strategies' sensitivity and efficiency mainly depend on the prevalence and the distribution of the Cq values. Our results indicate that both the prevalence and the Cq value distribution are dynamic parameters during the SARS-CoV-2 pandemic and that, as a result, the resulting sensitivity and efficiency of pooling strategies are as well. To enable researchers and institutions with a real-time and accessible recommendation concerning the optimal 1D pooling strategy for their testing population, we developed a Shiny app providing just that.

Two factors could explain the dynamics of the prevalence and the Cq value distribution: epidemiological and virological change within the same sampling population and variation in the sampling population. The existence of these factors would suggest that an intricate interplay of these two components is at the origin of the observed evolutions. Recent research indicated that the first component (epidemiological change) exists, as the distribution of random surveillance testing-deduced Cq values fluctuates during the SARS-CoV-2 pandemic (by definition, no changes in sampling population occurred in this research, thereby excluding this

factor from the equation)¹⁶. The second component (variation in sampling population) is bound to happen when the testing facility is not consistently receiving samples from the same origin, as is the case for Biogazelle. At the very introduction of Biogazelle as a testing facility, most samples originated from hospitals and sources were added progressively as the testing capacity increased. Additionally, the Belgian government instituted a rapid change in the testing regime on October 21st, 2020: only symptomatic suspected SARS-CoV-2 cases get tested. The federal government lifted this measure on November 23rd, 2020, when the number of cases lowered and the existing testing capacity sufficed again. Since symptomatic patients generally show lower Cq values^{17,18}, it is clear that sampling bias will contribute to the overall Cq value distribution.

The influence these dynamic parameters have on the variation of performance of pooling strategies is significant. This observation raises an issue for interpreting pooling strategy evaluations not based on time-series datasets. The effectiveness of a chosen pooling plan might even decrease to such an extent that it becomes inferior to individual testing. We observed this situation at the end of the second wave when efficiency is close to 1, but sensitivity is not (Figure 3). Based on these results, it becomes essential to regularly re-evaluate an adopted pooling strategy to avoid compromising on sensitivity and efficiency when there is no need.

Multiple effects contribute to how the testing population's characteristics drive pooling strategy outcomes. The main trends show that the prevalence mainly influences efficiency, and the Cq value distribution mainly influences sensitivity (Figure 3). We can explain both observations by using common sense and basic mathematics. When the prevalence is low, the efficiency is high: fewer pools will have positive samples and therefore test negative, which will automatically result in a lower number

of tests needed to test all samples. Additionally, when a considerable proportion of samples have a Cq value close to the single-molecule Cq value, a more significant fraction of samples will become too diluted to detect during pooling and result in false negatives. There appear to be secondary compensating effects of the Cq value distribution and prevalence on the efficiency and sensitivity, respectively, which are more subtle. Primarily, as a higher fraction of positive samples has a Cq value close to the upper limit, more pools will test (false) negative, boosting the efficiency. On the other hand, when the prevalence increases, the sensitivity will increase due to an effect we call 'rescuing': a high Cq value that would otherwise test negative when diluted in the pool is 'rescued' by a low Cq value in the same pool. When the prevalence rises, the chances of this phenomenon happening also increase and as will the sensitivity. The same was observed by Cleary et al.¹⁹. Although minor, these secondary effects explain a number of our observations.

To elaborate how the optimal pooling strategy (best efficiency trade-off) transforms over time, assume two situations: low prevalence and high prevalence. When the prevalence is low, the larger pool sizes will result in higher efficiency and lower prevalence (more dilution). However, when the prevalence is high, the 'rescuing' effect will be more prominent and counteract the increasing efficiency and decreasing sensitivity. These results are in line with the widely accepted idea that sample pooling methods show a higher efficiency when pool size is large and that as prevalence increases, it reached a threshold after which smaller pool sizes become more efficient^{1,9}. Intuitively, the 'rescuing' effect is less prominent in 2D pooling strategies, as both pools (row and column) need to rescue the high Cq sample.

False negatives have pre-pool Cq values close to the detection limit and predominantly originate from patients who are at the end of an infection^{19,20}, putting

387 their clinical relevance in question (i.e. no longer infectious). Similarly, however, one
388 can argue that these high Cq samples are imperative to a favorable pandemic
389 response: they might originate from pre-symptomatic or very recently-infected
390 patients¹⁹, allowing for catching cases before transmission—a principle at the very
391 core of every population screening strategy. Also, we cannot rule out that these high
392 Cq values are due to imperfect sampling or any other mistakes along the sample
393 preparation¹³.

394 Our study suffers from some essential limitations. First, although the data grouped by
395 weeks provides many different situations to assess, there will still be other
396 combinations of parameters that we did not analyze in this paper. However, the
397 current dataset probably represents the most plausible scenarios as the data
398 originates from a protracted period of the pandemic. Second, we selected only 1D
399 and 2D pooling methods in this simulation study. As stated before, other pooling
400 regimes exist and might be more performant than the discussed ones. Yet, these
401 pooling strategies come with intrinsic shortcomings. The P-BEST pooling protocol is
402 very time consuming¹⁰, even when using a pipetting robot, and the repeated pooling
403 method suffers from a complicated re-pooling scheme¹. Third, our model relies on
404 the critical assumption that we can directly induce the pool's Cq value from the
405 individual samples' Cq values using a simple formula (see Methods). Wet lab
406 experiments have shown that this is not necessarily the case⁵⁻⁸. Fourth, to calculate
407 the pooling strategies' performance, the single-molecule Cq value and the
408 prevalence must be known. However, we can easily calculate the single-molecule Cq
409 value by generating a ddPCR calibrated dilution series as done in this paper. The
410 prevalence, however, cannot be known precisely, and as a result, the prevalence
411 must be estimated. We can do this either before adopting a pooling strategy by

testing the individual samples and using the fraction of positive samples as an indication for the prevalence or when a pooling strategy is already in place by calculating it from the percentage of positive pools^{2,19}. Last, the calculated efficiency gain is merely a representation of the number of individual RNA extractions and RT-qPCR reactions and does not evaluate the amount of labor or time-to-result. Pooling a low number of samples will unnecessarily increase the time-to-result and workload. In conclusion, we show that finding the optimal pooling strategy for SARS-CoV-2 test samples is guided by a testing population-dependent efficiency-sensitivity trade-off. Consequently, the most favorable pooling regime might change throughout the pandemic due to epidemiological changes and revisions in diagnostic testing strategies. We provide an accessible shiny application to guide readers towards the optimal pooling strategy to fit their needs.

Acknowledgements

We are grateful for the data from the Belgian federal taskforce for COVID-19 qPCR testing.

Conceptualization: J.Va., P.M. and J.Ve.; Methodology: J.Va., P.M. and J.Ve.; Software: J.Ve., T.S.; Formal Analysis: J.Ve.; Resources: J.H., J.Va. and P.M.; Data Curation: J.Ve.; Writing – Original Draft: J.Va. and J.Ve.; Writing – Review & Editing: J.Va., J.H., P.M., T.S. and J.Ve.; Visualisation: J.Va. and J.Ve.; Supervision: J.Va. and P.M.; Project Administration: J.Va. and P.M.

Data availability

436 The code and Cq values are available on
437 <https://github.com/OncoRNALab/covidpooling>.

References

1. Shani-Narkiss H, Gilday OD, Yayon N, Landau ID. Efficient and Practical Sample Pooling High-Throughput PCR Diagnosis of COVID-19. MedRxiv, 2020:2020.04.06.20052159
2. Guha P, Guha A, Bandyopadhyay T. Application of pooled testing in screening and estimating the prevalence of Covid-19. MedRxiv, 2020:2020.05.26.20113696
3. Adams K. Expanding Covid-19 Testing: Mathematical Guidelines for the Optimal Sample Pool Size Given Positive Test Rate. MedRxiv, 2020:2020.05.21.20108522
4. Million R, Mortarino C. Sequential informed pooling approach to detect SARS-CoV2 infection. MedRxiv, 2020:2020.04.24.20077966
5. Hogan CA, Sahoo MK, Pinsky BA. Sample Pooling as a Strategy to Detect Community Transmission of SARS-CoV-2. JAMA - J Am Med Assoc, 2020, 323:1967–9
6. Yelin I, Aharony N, Shaer Tamar E, Argoetti A, Messer E, Berenbaum D, Shafran E, Kuzli A, Gandali N, Shkedi O, Hashimshony T, Mandel-Gutfreund Y, Halberthal M, Geffen Y, Szwarcwort-Cohen M, Kishony R, Taub Professor H. Evaluation of COVID-19 RT-qPCR test in multi-sample pools. Clin Infect Dis, 2020. <https://doi.org/https://doi.org/10.1093/cid/ciaa531>
7. Abdalhamid B, Bilder CR, McCutchen EL, Hinrichs SH, Koepsell SA, Iwen PC. Assessment of Specimen Pooling to Conserve SARS CoV-2 Testing Resources. Am J Clin Pathol, 2020, 153:715–8
8. Torres I, Albert E, Navarro D. Pooling of nasopharyngeal swab specimens for SARS-CoV-2 detection by RT-PCR. J Med Virol, 2020, 92:2306–7

- 463 9. Sinnott-Armstrong N, Klein D, Hickey B. Evaluation of Group Testing for SARS-
464 CoV-2 RNA. MedRxiv, 2020:2020.03.27.20043968
- 465 10. Shental N, Levy S, Wuvshet V, Skorniakov S, Shalem B, Ottolenghi A,
466 Greenshpan Y, Steinberg R, Edri A, Gillis R, Goldhirsh M, Moscovici K,
467 Sachren S, Friedman LM, Nesher L, Shemer-Avni Y, Porgador A, Hertz T.
468 Efficient high-throughput SARS-CoV-2 testing to detect asymptomatic carriers.
469 Sci Adv, 2020, 6:5961–72
- 470 11. Ghosh S, Agarwal R, Rehan MA, Pathak S, Agrawal P, Gupta Y, Consul S,
471 Gupta N, Goyal R, Rajwade A, Gopalkrishnan M. A Compressed Sensing
472 Approach to Group-testing for COVID-19 Detection. ArXiv, 2020
- 473 12. Gan Y, Du L, Damola FO, Huang J, Xiao G, Lyu X. Sample Pooling as a
474 Strategy of SARS-COV-2 Nucleic Acid Screening Increases the False-negative
475 Rate. MedRxiv, 2020:2020.05.18.20106138
- 476 13. Dahdouh E, Lázaro-Perona F, Romero-Gómez MP, Mingorance J, García-
477 Rodriguez J. Ct values from SARS-CoV-2 diagnostic PCR assays should not
478 be used as direct estimates of viral load. J Infect, 2020.
479 <https://doi.org/10.1016/j.jinf.2020.10.017>
- 480 14. Buchan BW, Hoff JS, Gmehlin CG, Perez A, Faron ML, Munoz-Price LS,
481 Ledebor NA. Distribution of SARS-CoV-2 PCR cycle threshold values provide
482 practical insight into overall and target-Specific sensitivity among symptomatic
483 patients. Am J Clin Pathol, 2020. <https://doi.org/10.1093/AJCP/AQAA133>
- 484 15. Corman VM, Landt O, Kaiser M, Molenkamp R, Meijer A, Chu DK, Bleicker T,
485 Brünink S, Schneider J, Schm ML, Mulders DG, Haagmans BL, van der Veer
486 B, van den Brink S, Wijsman L, Goderski G, Romette J-L, Ellis J, Zambon M,
487 Peiris M, Goossens H, Reusken C, Koopmans MP, Drosten C. Detection of

488 2019 novel coronavirus (2019-nCoV) by real-time RT-PCR. Eurosurveillance,
489 2020, 25:2000045

490 16. Hay JA, Kennedy-Shaffer L, Kanjilal S, Lipsitch M, Mina MJ. Estimating
491 epidemiologic dynamics from single cross-sectional viral load distributions.
492 MedRxiv, 2020:2020.10.08.20204222

493 17. Singanayagam A, Patel M, Charlett A, Bernal JL, Saliba V, Ellis J, Ladhani S,
494 Zambon M, Gopal R. Duration of infectiousness and correlation with RT-PCR
495 cycle threshold values in cases of COVID-19, England, January to May 2020.
496 Eurosurveillance, 2020. [https://doi.org/10.2807/1560-](https://doi.org/10.2807/1560-7917.ES.2020.25.32.2001483)
497 7917.ES.2020.25.32.2001483

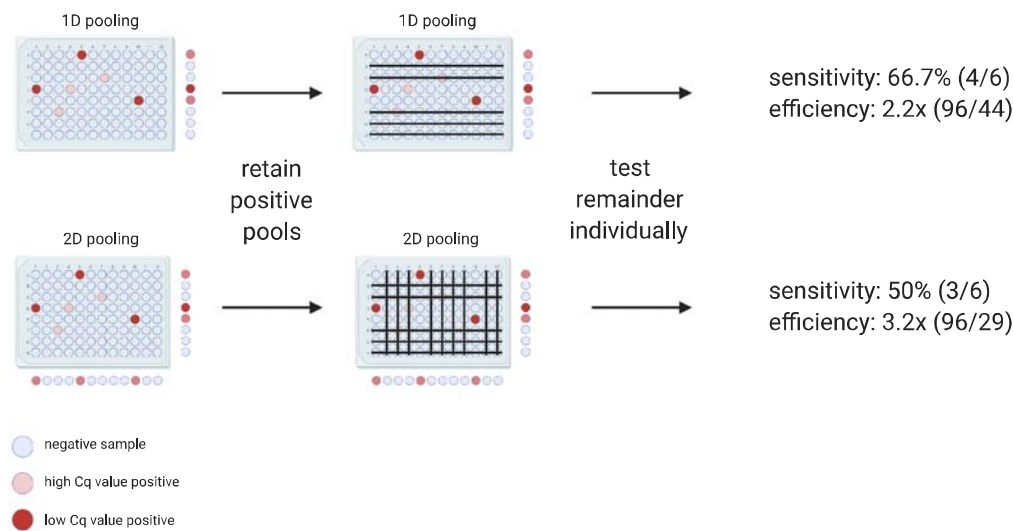
498 18. Gorzalski AJ, Hartley P, Laverdure C, Kerwin H, Tillett R, Verma S, Rossetto
499 C, Morzunov S, Hooser S Van, Pandori MW. Characteristics of viral specimens
500 collected from asymptomatic and fatal cases of COVID-19. J Biomed Res,
501 2020, 34:431–6

502 19. Cleary B, Hay JA, Blumenstiel B, Harden M, Cipicchio M, Bezney J, Simonton
503 B, Hong D, Senghore M, Sesay AK, Gabriel S, Regev A, Mina MJ. Using viral
504 load and epidemic dynamics to optimize pooled testing in resource-constrained
505 settings. Sci Transl Med, 2021:eabf1568

506 20. Tom MR, Mina MJ. To Interpret the SARS-CoV-2 Test, Consider the Cycle
507 Threshold Value. Clin Infect Dis, 2020, 71:2252–4
508
509

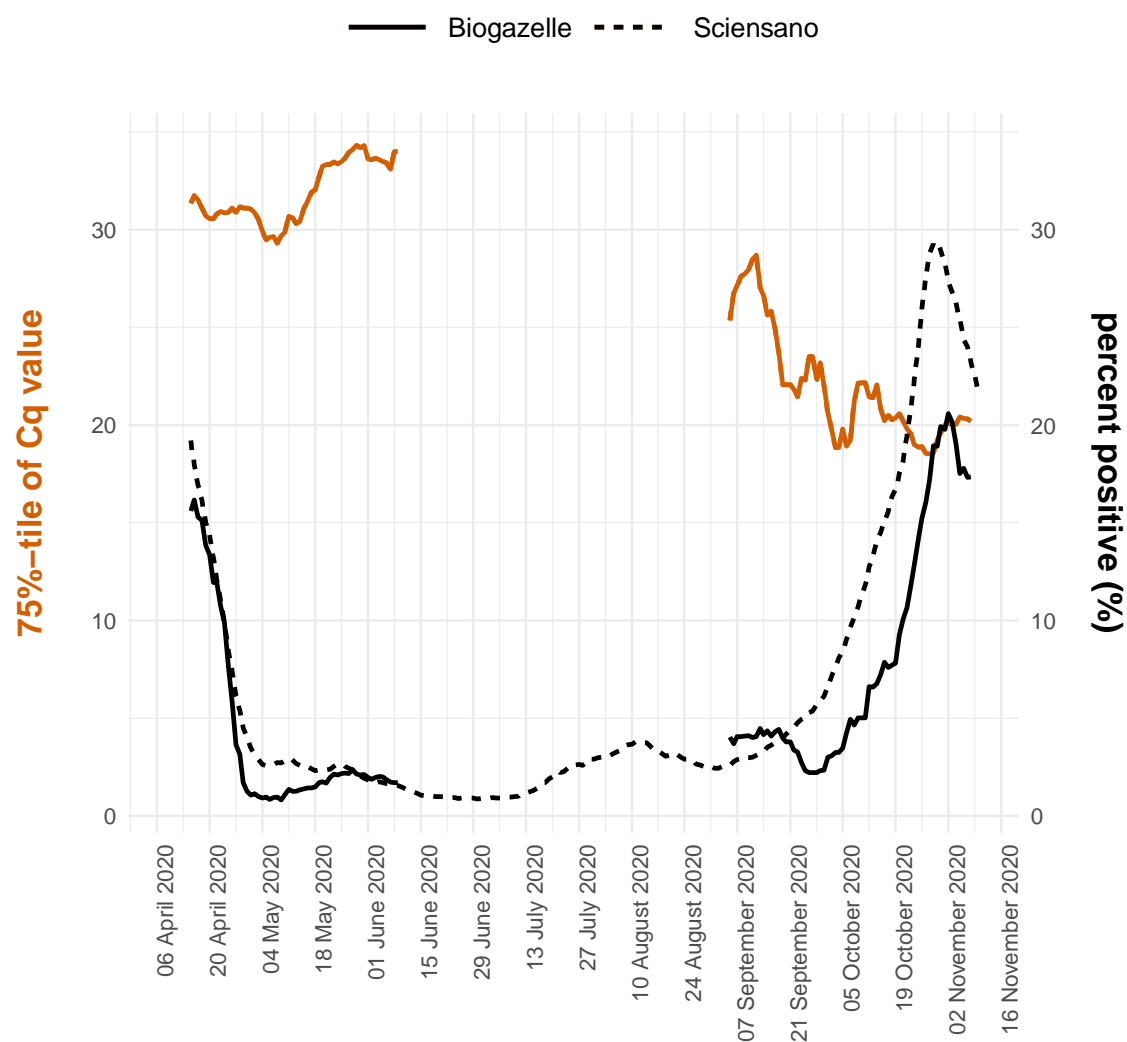
510 **Figures**

511 **Figure 1**



512

513 **Figure 2**



514

515 **Figure 3**

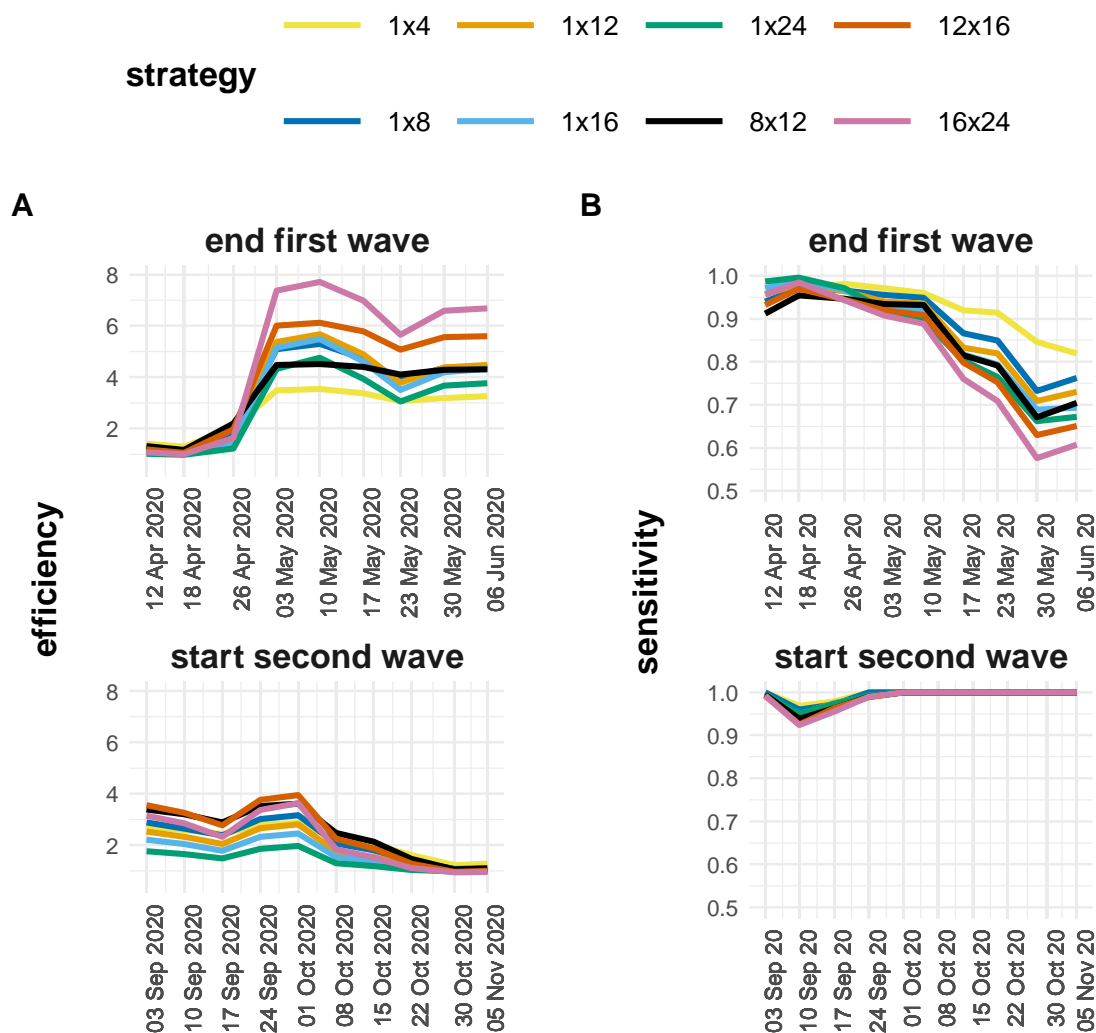


Figure 4

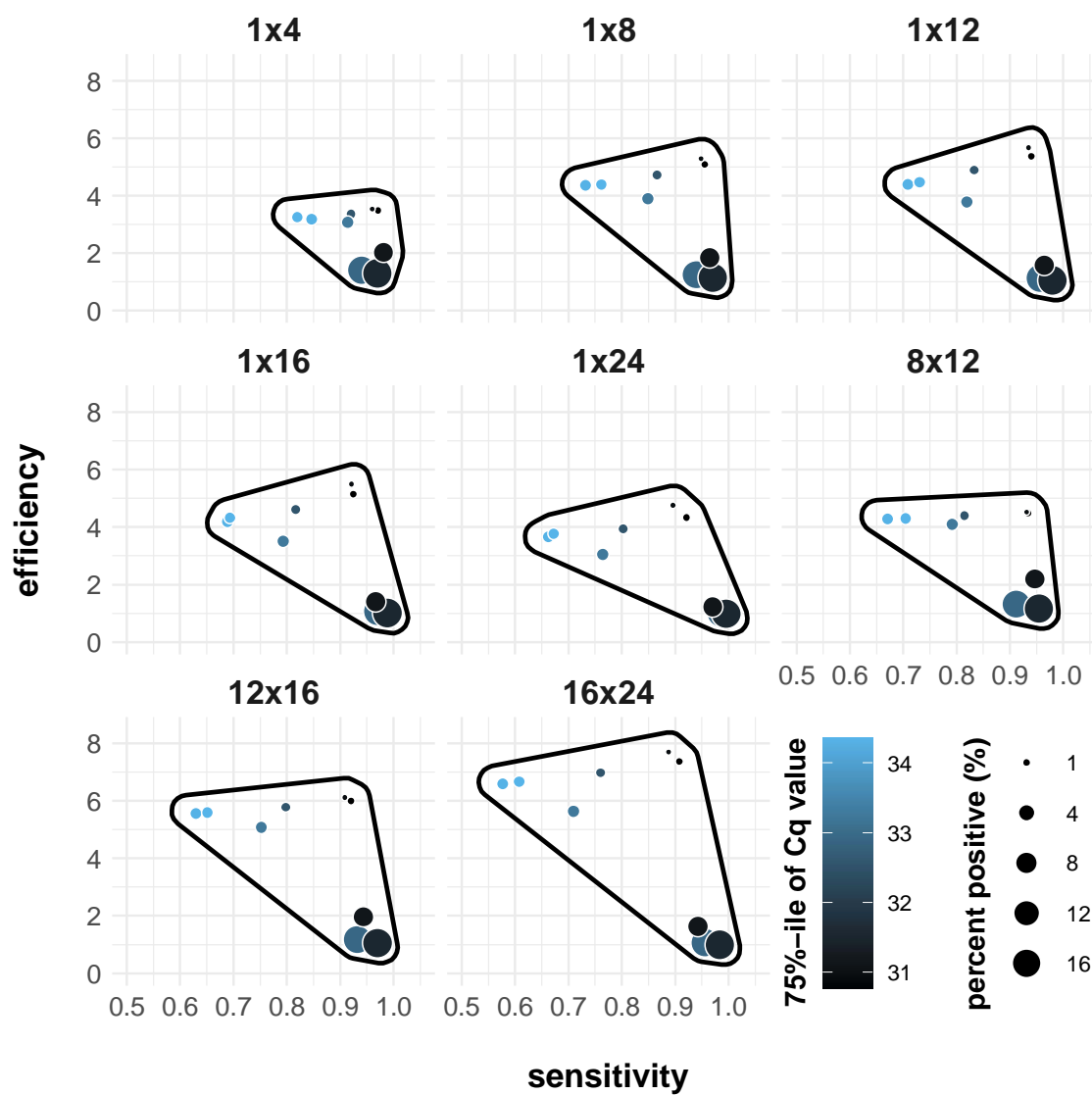


Figure Legends

Figure 1: Schematic overview of the applied pooling strategies. The samples are represented as wells in a 96-well microtiter plate. The color of the wells indicates the samples' SARS-CoV-2 RNA concentration. In 1D pooling, the pools are created by row, the pools are tested and the samples in positive pools are tested again individually. During 2D pooling, the pools are created by row and column (each sample exists in two pools), the pools are tested, all negative rows and columns are removed and the remaining samples are tested individually. The sensitivity and the efficiency are calculated according to the equations found in the methods.

Figure 2: Evolution of the 75%-tile of the Cq value distribution and fraction of positive samples. The left y-axis shows the seven day moving window average of the 75%-tile of the Cq value distribution of the data originating from Biogazelle and the right y-axis shows the seven day moving window average of the fraction of positive samples for the Biogazelle and Sciensano data. The two datasets are differentiated by the line type. If the moving average was calculated using on the basis of less than five days (due to no data being available for specific days), the datapoint was removed from the visualization.

Figure 3: Sensitivity and efficiency for the end of the first (A) and the start of the second (B) Belgian SARS-CoV-2 infection wave. The data is grouped by week and the sensitivity and efficiency are calculated by simulating different pooling strategies (1x4, 1x8, 1x12, 1x16, 1x24, 8x12, 12x16 and 16x24). The pooling strategies can be distinguished by color.

Figure 4: Simulated sensitivity and efficiency for the end of the first wave visualized with relation to the week (different circles), fraction of positive samples (size of circles) and 75%-tile of the Cq value distribution (color). A polygon is drawn around the datapoints (with a small margin) to visualize and to compare the variability of the sensitivity and efficiency over a period of time between pooling strategies.

**Supplemental Information to *Evaluation of efficiency and sensitivity*
of 1D and 2D sample pooling strategies for SARS-CoV-2 RT-qPCR
screening purposes**

**Jasper Verwilt^{1,2,3}, Jan Hellemans⁴, Tom Sante^{2,3}, Pieter Mestdag^{1,2,3,4}, Jo
Vandesompele^{1,2,3,4}**

*1 OncoRNALab, Cancer Research Institute Ghent, Corneel Heymanslaan 10, 9000
Ghent, Belgium*

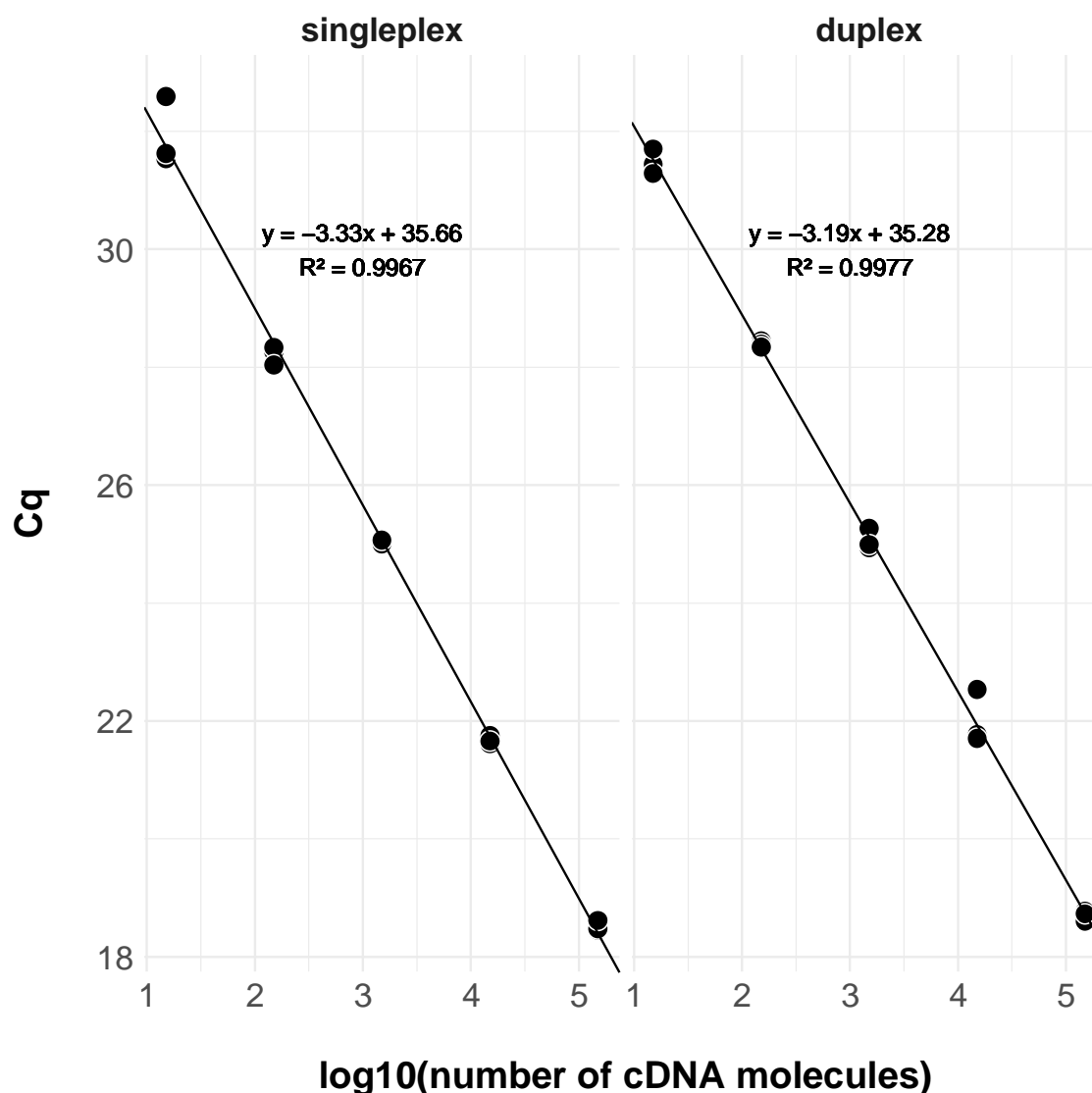
*2 Department of Biomolecular Medicine, Ghent University, Corneel Heymanslaan 10,
9000 Ghent, Belgium*

*3 Center for Medical Genetics, Ghent University, Corneel Heymanslaan 10, 9000
Ghent, Belgium*

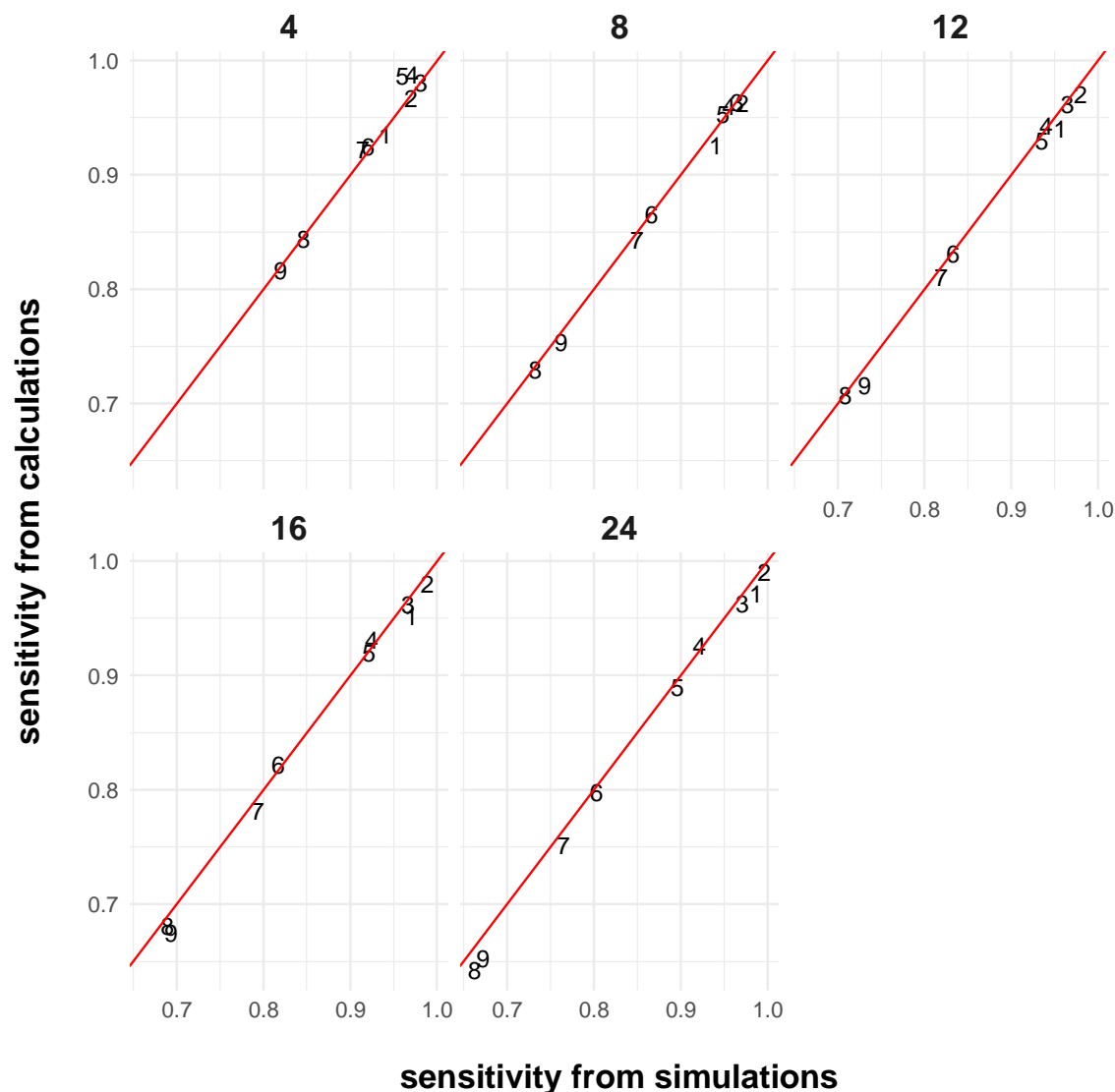
4 Biogazelle, Technologiepark-Zwijnaarde 82, 9052 Gent, Belgium

- 4 supplemental figures

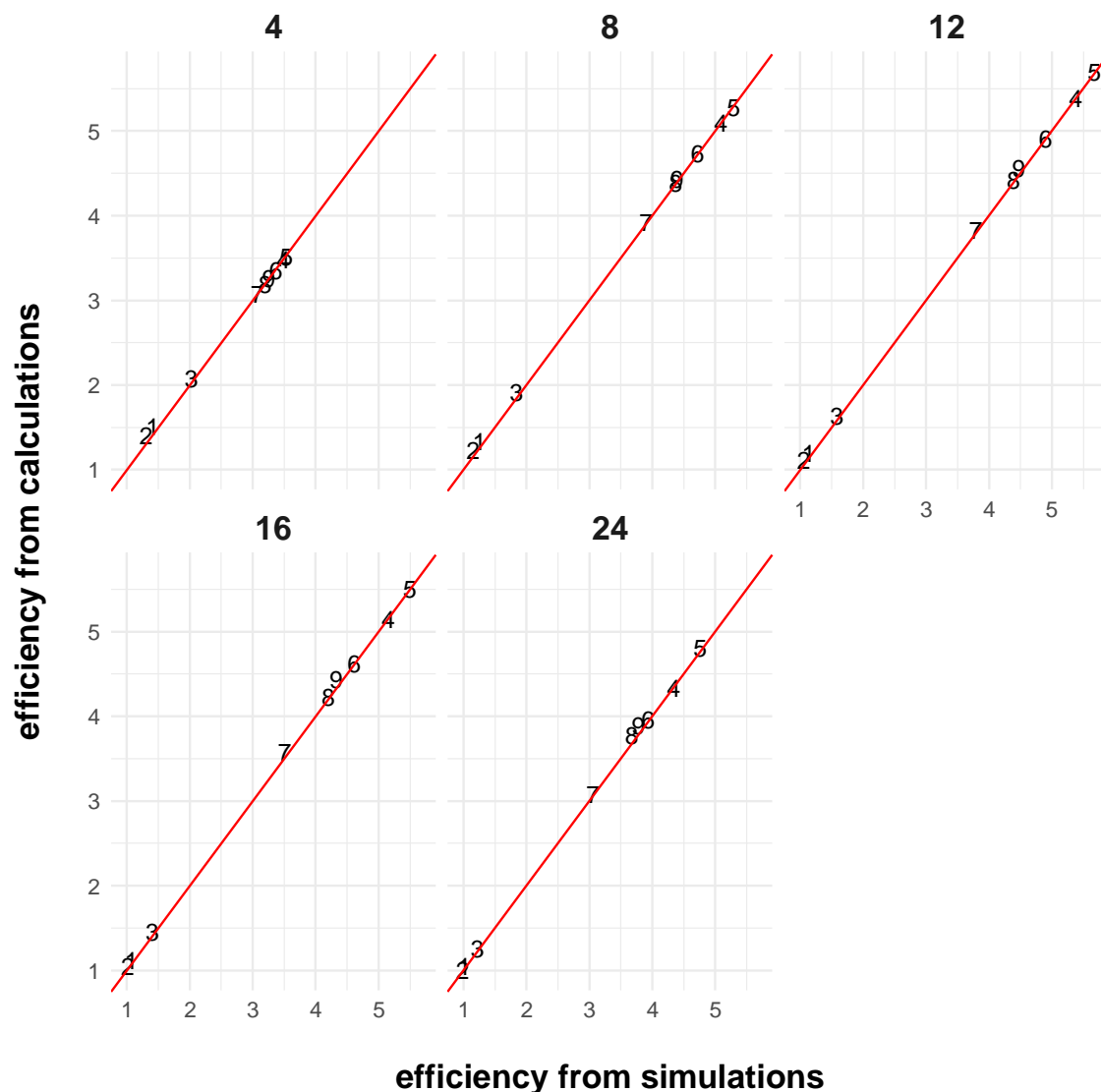
Supplemental Figures



Supplemental Figure 1: Sensitivity analysis of singleplex and duplex qPCR assays using predetermined number of cDNA molecules. R-squared values are adjusted using the Wherry formula. Each number of cDNA molecules was tested in triplicate.



Supplemental Figure 2: Concordance of sensitivity estimations between simulations and calculations for the end of the first Belgian SARS-CoV-2 infection wave. The numbers represent the weeks (1: 1st week; 2: 2nd week; ...) and are plotted at the sensitivities derived from the simulations and calculations. The red line represents the points where both values are equal.



588

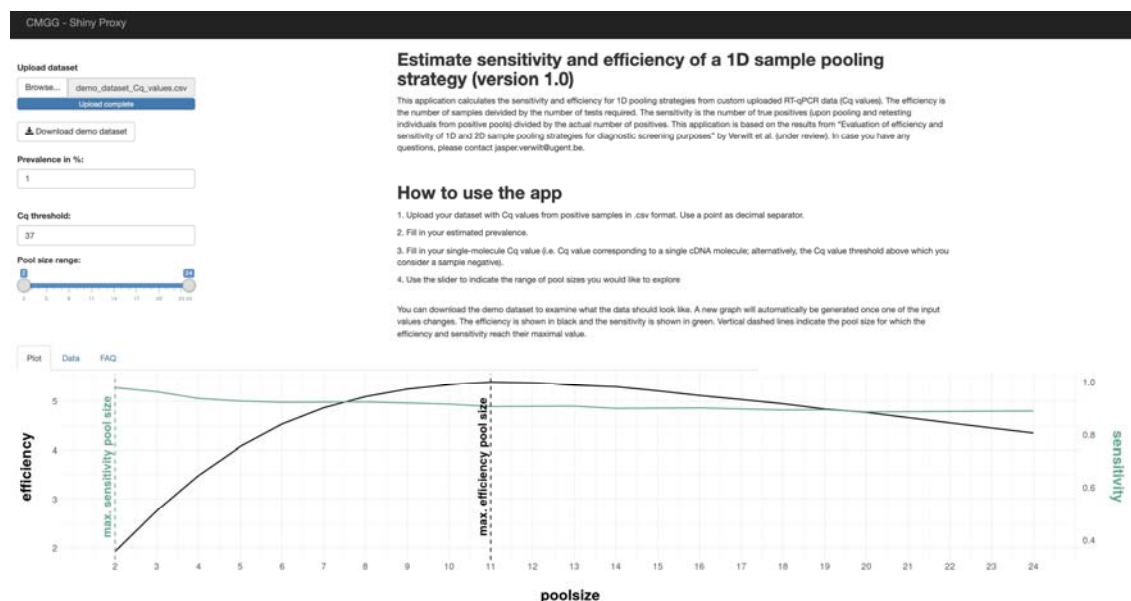
589 **Supplemental Figure 3:** Concordance of efficiency estimations between simulations and calculations

590 for the end of the first Belgian SARS-CoV-2 infection wave. The numbers represent the weeks (1: 1st

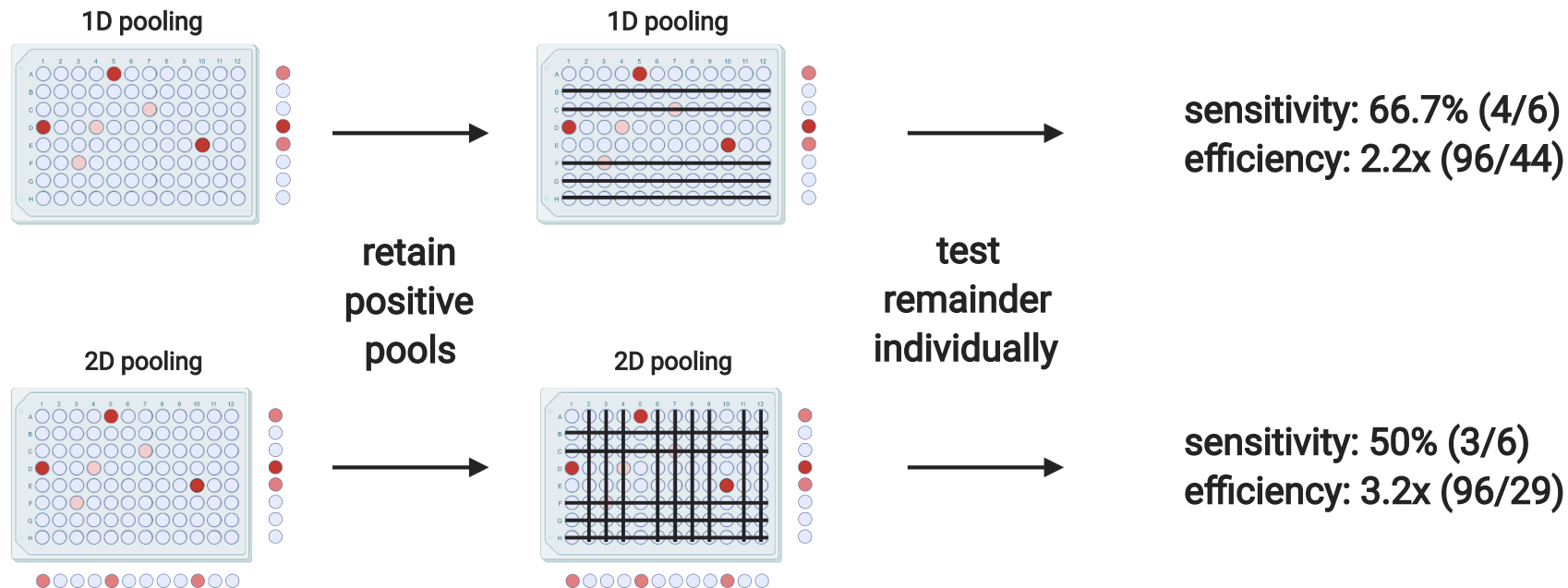
591 week; 2: 2nd week; ...) and are plotted at the efficiencies derived from the simulations and calculations.




592 The red line represents the points where both values are equal.

593



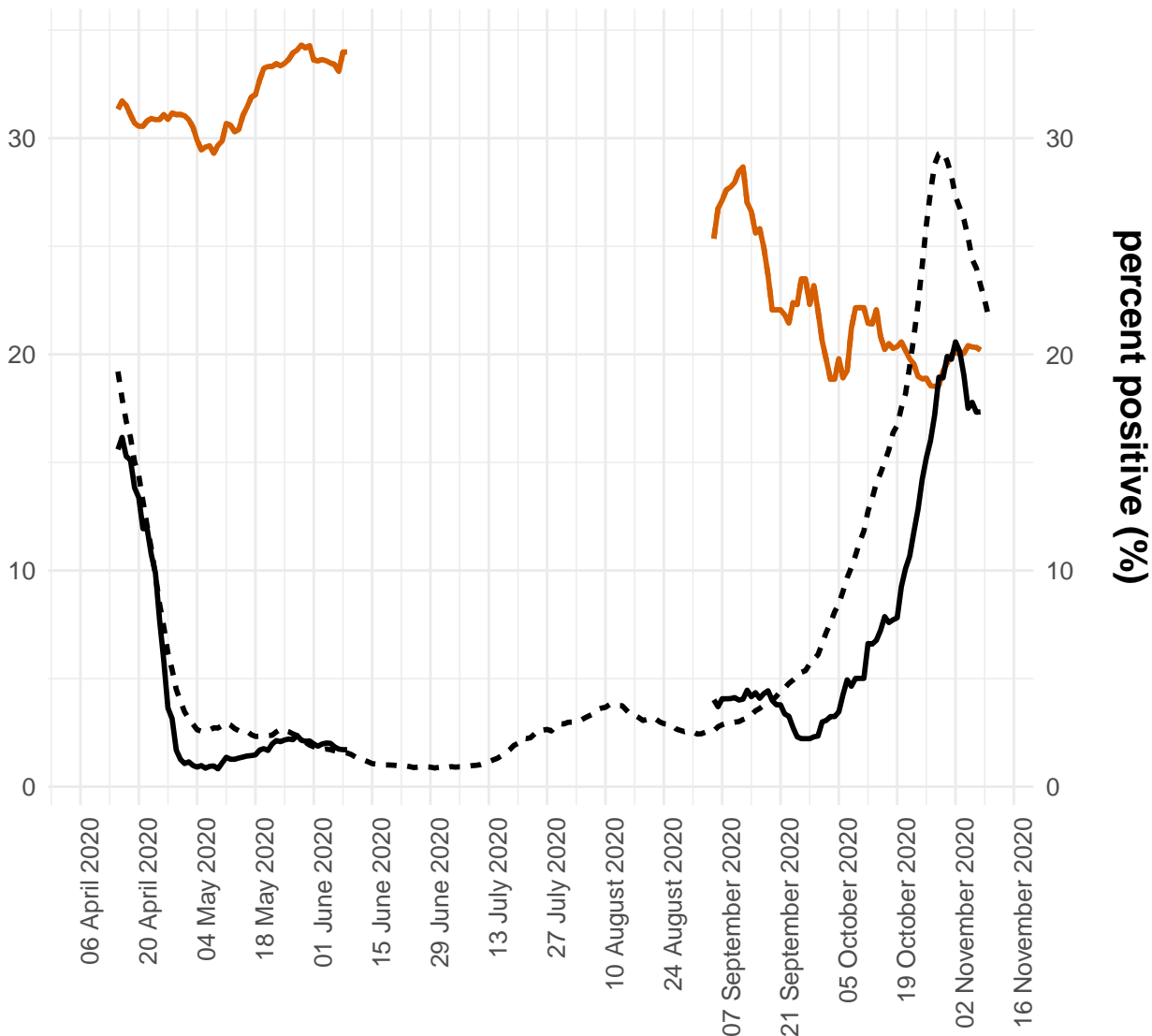
Supplemental Figure 4: A screenshot of the interface of the Shiny application. The webpage provides the user with a short description and a detailed outline of how to use the application. In the upper left corner, the user can provide their dataset. If the user would prefer to first explore the app without using their own data, a demo dataset can be downloaded and used instead. The user can fill in the estimated prevalence and single-molecule Cq value. The slider underneath can be used to indicated which range of pool sizes the user wishes to explore. Upon uploading the data, a graph will be outputted in the "Plot" tab, showing the estimated sensitivity and efficiency of each pool size. The vertical dashed lines represent the pool size at which the corresponding parameter reaches its maximal value for this data. The "Data" tab provides the user with a tabulated overview of the estimated sensitivity and efficiency of each pool size.



-  negative sample
-  high Cq value positive
-  low Cq value positive

75%-tile of Cq value

— Biogazelle - - - Sciensano



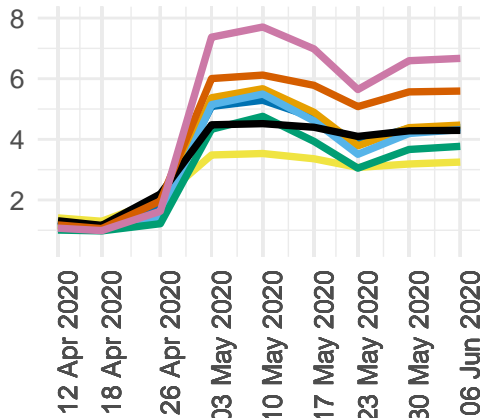
strategy

1x4 1x12 1x24 12x16

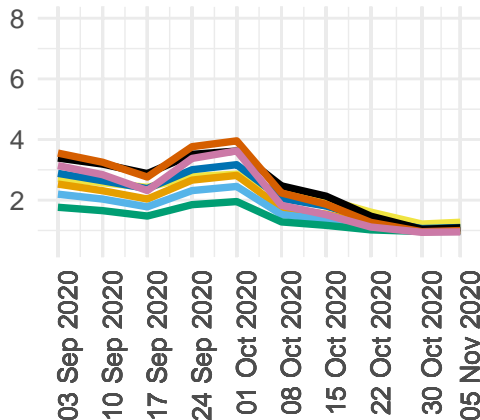
1x8 1x16 8x12 16x24

A

end first wave

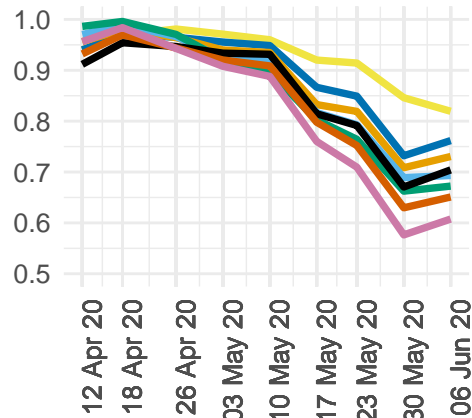


start second wave

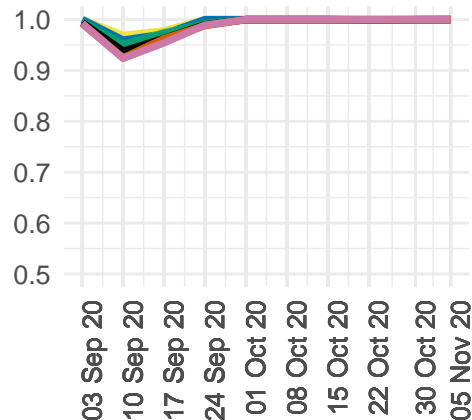


B

end first wave

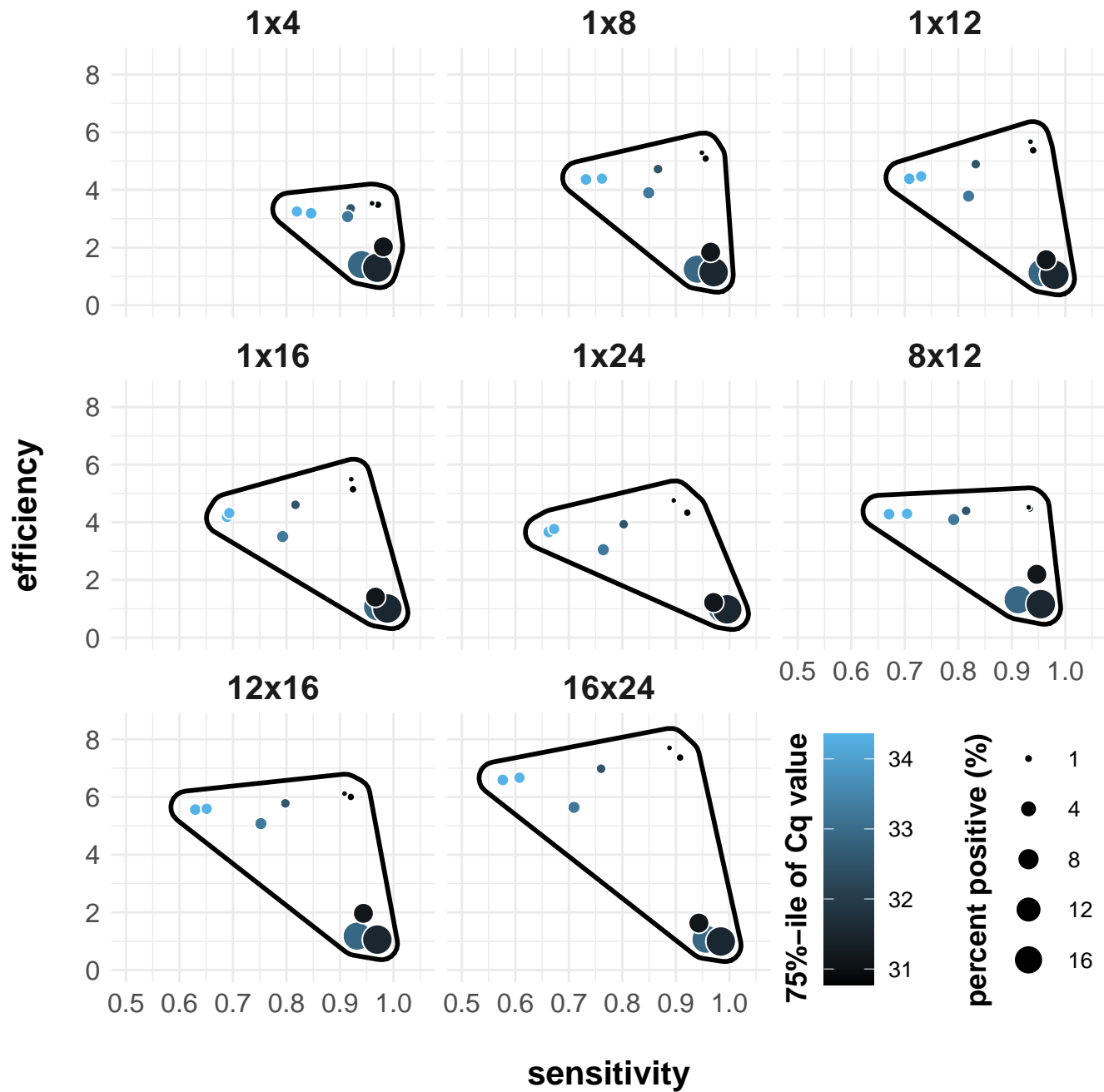


start second wave



efficiency

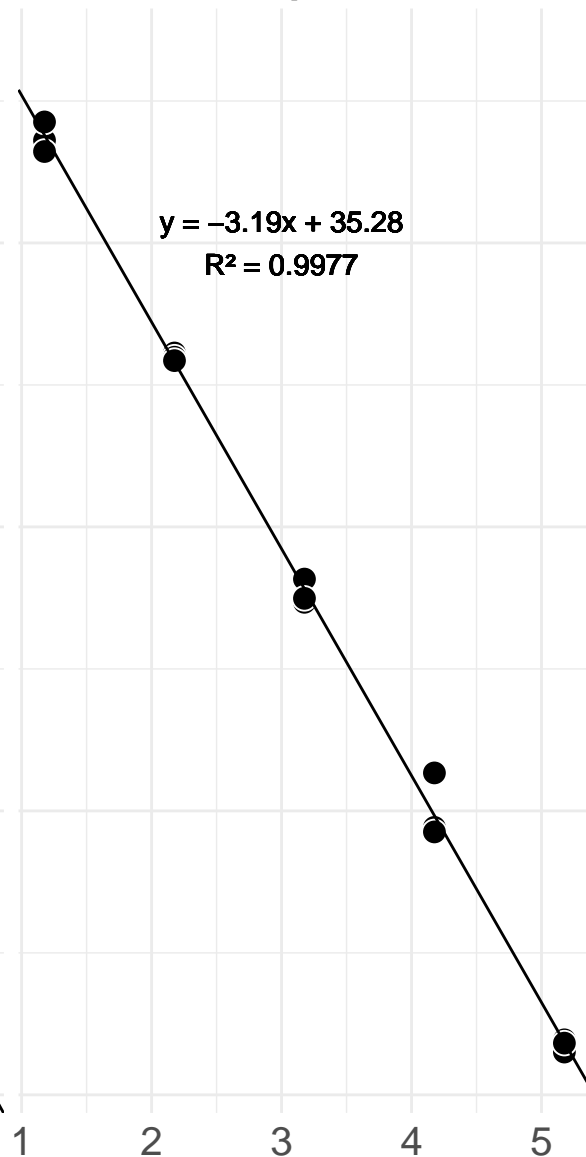
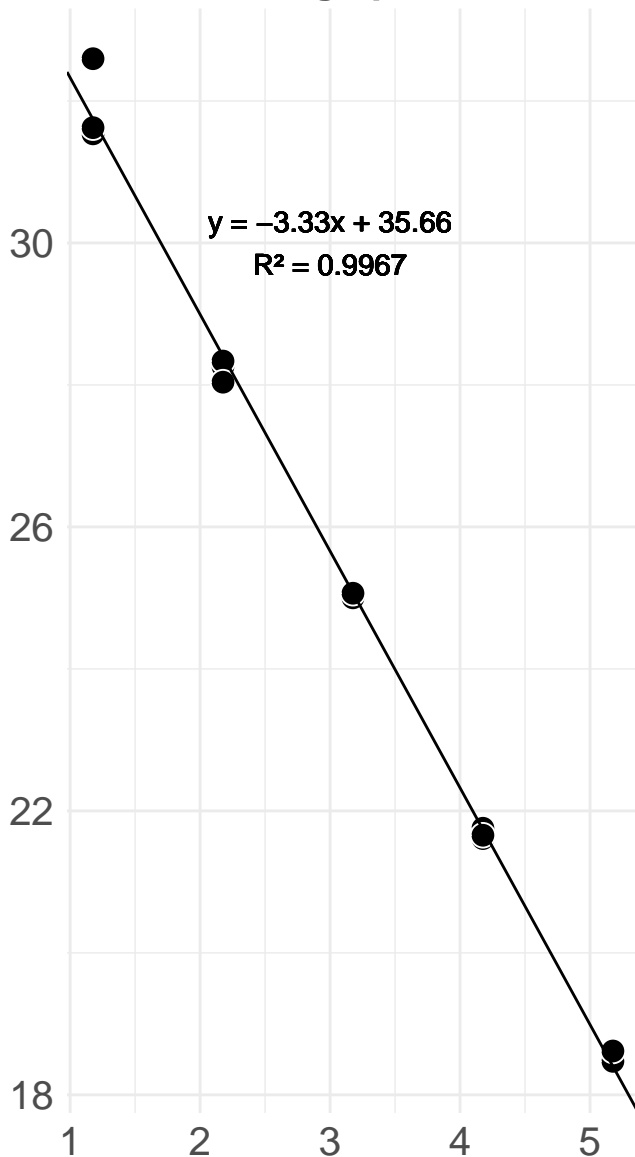
sensitivity



singleplex

duplex

Cq



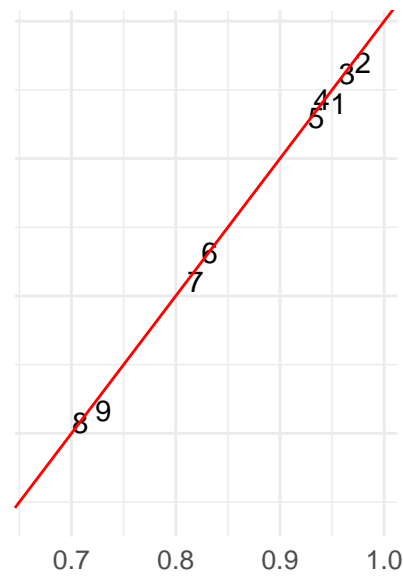
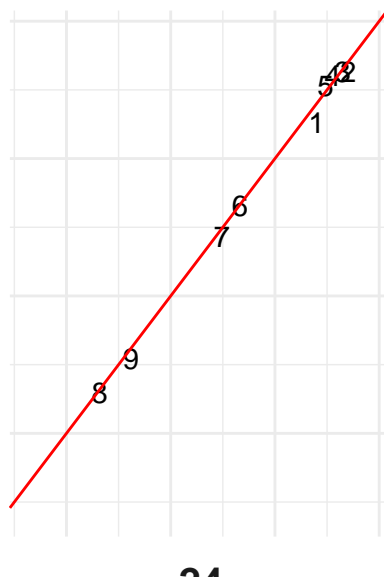
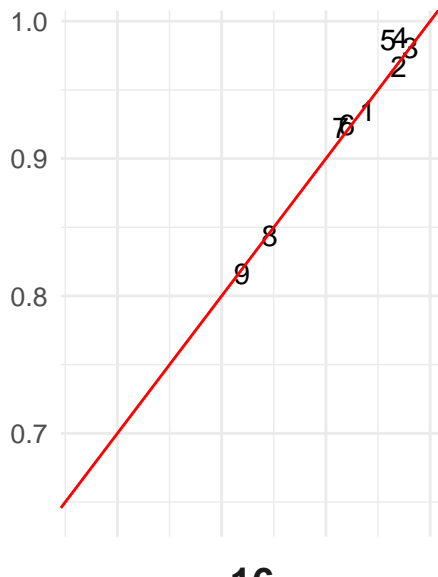
log10(number of cDNA molecules)

sensitivity from calculations

4

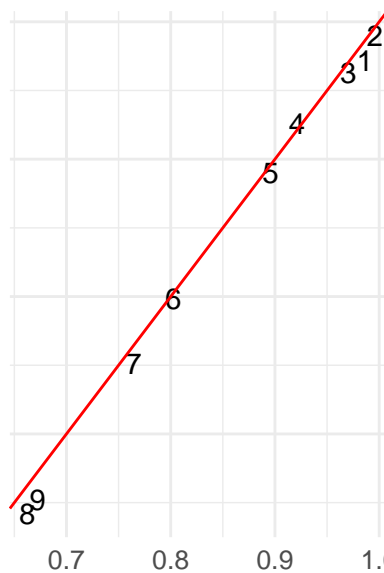
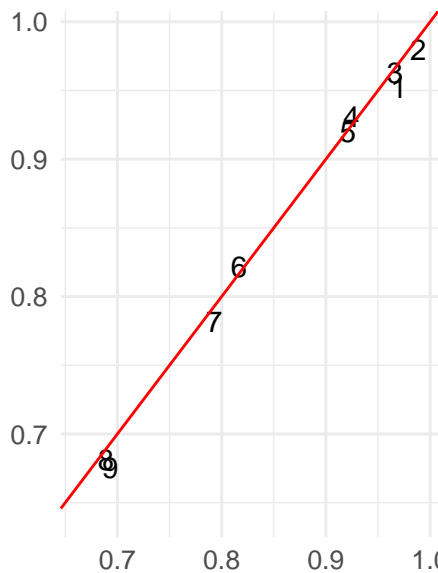
8

12



16

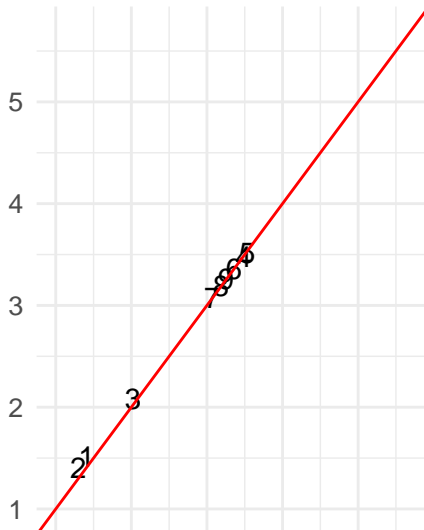
24



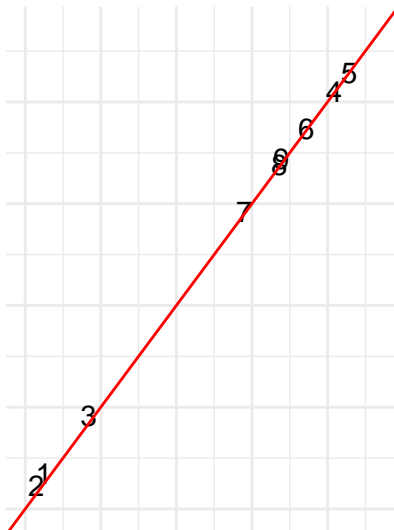
sensitivity from simulations

efficiency from calculations

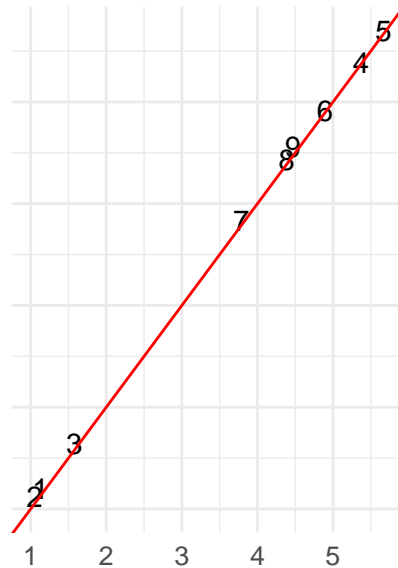
4



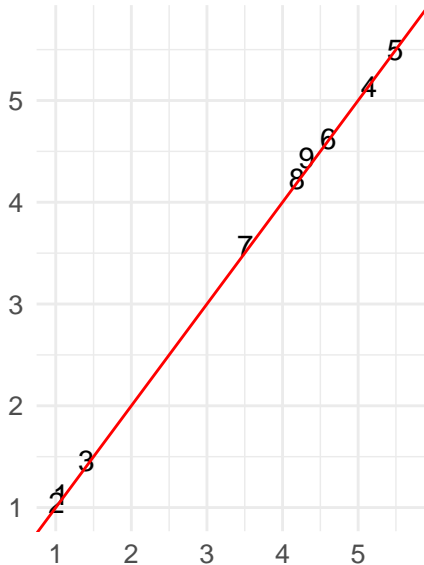
8



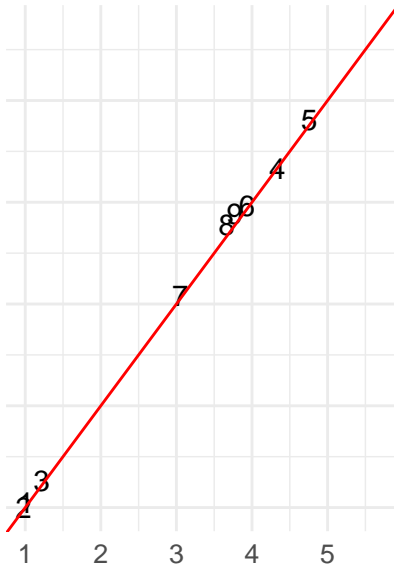
12



16



24



efficiency from simulations

Upload dataset

Browse...

demo_dataset_Cq_values.csv

Upload complete

Download demo dataset

Prevalence in %:

1

Cq threshold:

37

Pool size range:

2

24

medRxiv preprint doi: <https://doi.org/10.1101/2020.07.17.20152702>; this version posted April 15, 2021. The copyright holder for this preprint (which was not certified by peer review) is the author/funder, who has granted medRxiv a license to display the preprint in perpetuity. It is made available under a CC-BY-NC 4.0 International license.

